NUMERICAL STUDY OF FULL-WIDTH, RHS-TO-RHS, X-CONNECTIONS UNDER TRANSVERSE COMPRESSION

JENS KUHN[1]

[1]*schlaich bergermann partner, Schwabstrasse 43,70197 Stuttgart, Germany.*
E-mail: jens.kuhn@sbp.de

This paper presents an investigation into full-width, RHS X-connections failing either by web buckling or yielding, taking tensile and compressive prestress in the chord into account. A recent re-evaluation of world-wide, tested, full-width X-connections revealed considerable inaccuracy with current design recommendations, as well as significant discrepancies between them. A finite element (FE) research program was hence conducted to further investigate the connection behaviour of full-width, RHS-to-RHS, X-connections under transverse compression with a focus on the effect of a compressive or tensile chord preload. A critical value for the $(h_1/\sin\theta_1)/h_0$ ratio was found, at which a transition from a failure mode of web yielding to web buckling failure occurs. The proposed design procedure is verified against 350 (152 valid tests, in the range of validity) finite element results covering a wide range of chord sidewall slenderness values, bearing length values and chord stress ratios, as well as against a data base of 51 prior experimental tests, and is proven to offer excellent predictions. Finally, the Eurocode "standard evaluation procedure" (method (a)) was performed to ensure that the proposed equation possesses the required level of safety. The proposed design method herein gives an accurate, safe and economical recommendation.

Keywords: Steel structures, hollow structural sections, rectangular hollow sections, truss connections, welded joints, web buckling, web crippling, static strength, numerical modelling.

1 Introduction

A great deal of recent research has focused on the behavior of welded rectangular hollow sections (RHS) under predominantly static loads. The results have led to several internationally recognized design recommendations, such as ISO 14346 (ISO 2013), CIDECT Design Guide No. 3, 2nd edition (Packer et al. 2009) and Wardenier et al. (2010) and are prescribed by prominent normative codes such as EN 1993-1-8 (CEN 2005a) and AISC 360-16 (2016).

Recently, the experimental database of compression-loaded, full-width, RHS-to-RHS X-connections has been re-visited and expanded (Fan 2017), and evaluated against contemporary design standards. This has revealed that current standards in North America (AISC 2016; CSA 2014) are often unsafe, yet Eurocode 3 (CEN 2005a) and CIDECT design recommendations (Packer et al. 2009) give safe but very uneconomical (excessively conservative) predictions. Since experimental investigations are expensive and time-consuming, numerical investigations are often carried out to generate a large additional database, which is the research topic of this paper. Thus, the numerical investigations cover compression as well as tension chord preloads. Further, the important influence of the bearing length (relative to the chord height) and the chord web slenderness on whether the chord web fails by buckling or yielding is studied detailed already shown by Davies and Packer (1987). Based on the experimental and numerical investigations a proposal is presented, which allows a safe and economic design of X-connections.

Proceedings of the 17th International Symposium on Tubular Structures.
Editors: X.D. Qian and Y.S. Choo

Published by Research Publishing, Singapore.
ISBN: 978-981-11-0745-0; doi:10.3850/978-981-11-0745-0_065-cd

2 Experimental Database

A database of 51 full-width welded, X-connections with branches under axial compression, assembled from prior experiments, is given in Fan (2017), plus the data for two additional tests in Fan (2017) is used to verify the numerical model. Source references for most tests are given in Fan (2017), but Kuhn (2018) additionally includes experiments by Cheng and Becque (2016), and Serrano et al. (2017). It is noted that this paper follows the established CIDECT nomenclature, where h_0 and h_1 are the chord height and the branch height, respectively, b_0 and b_1 represent the chord width and the branch width, respectively, and t_0 and t_1 refer to the thicknesses of the chord and the branch (Fig. 1).

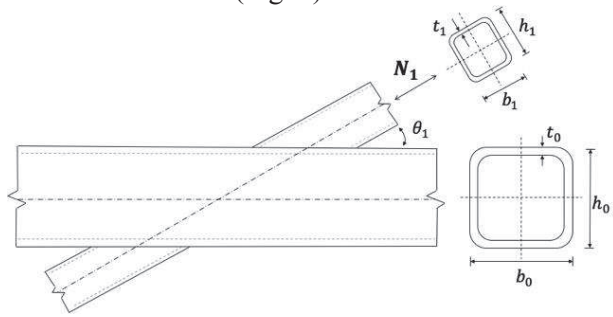

Figure 1. Notation for RHS-to-RHS welded X-connections

3 Finite Element Modelling

To validate the finite element (FE) modelling procedure used herein, two RHS-to-RHS full-width X-connection FE models were developed using ANSYS v18 (Swanson Analysis Systems 2017). The finite element model was first bench-marked against two experimental results involving equal-width RHS X-connections, with a branch welded only on one side of the chord and supported by a steel pedestal, with no chord preload applied, obtained from Fan (2017).

Table 1. Measured dimensions

Label	Nominal branch size	Chord						Material	
		h_0 [mm]	b_0 [mm]	t_0 [mm]	r_i [mm]	r_o [mm]	l_0 [mm]	f_y [MPa]	f_u [MPa]
X-1.0-32-700O	203x203x6.35	203.60	203.60	5.96	14.98	8.99	1603	388.8	508.7
X-1.0-21-550O	203x203x9.53	203.10	203.10	8.85	23.82	14.98	1303	398.1	519.8
Label	**Nominal branch size**	**Branch**						**Weld**	
		h_1 [mm]	b_1 [mm]	t_1 [mm]	r_i [mm]	r_o [mm]	l_1 [mm]	a_w [mm]	
X-1.0-32-700O	203x203x12.7	204	204	11.67	32.67	21.04	808	6.80	
X-1.0-21-550O	203x203x12.7	204	204	11.67	32.67	21.04	808	6.90	

The model incorporated the experimentally-measured dimensions and weld sizes, the values of which can be found in Table 1 and in Fan (2017). Material properties obtained from three coupon test results were included in the model. Note that the stress-strain curves in Fig.2 are engineering stresses.

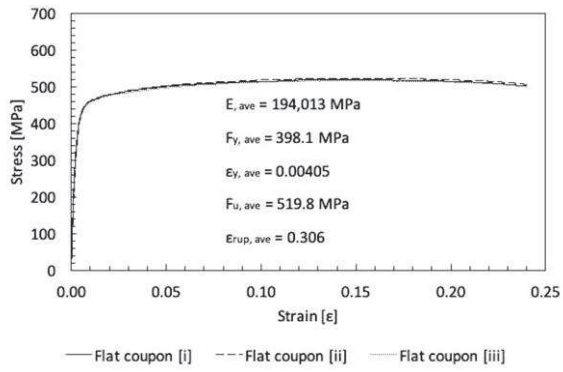

Figure 2. Engineering stress-strain curves for 3 coupon tests, adapted from Fan (2017)

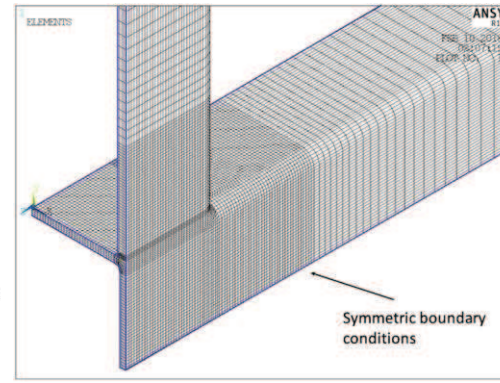

Figure 3. One-eighth model used for RHS-to-RHS welded X-connections

Planes of symmetry were used, to reduce the number of degrees of freedom. For modelling the two "welded on one side" test specimens, quarter models were used. For the subsequent parametric analysis of "welded" (branches welded on both sides of the chord) RHS-to-RHS X-connections, the model was cut in the middle of the chord web and an additional symmetric plane was added. Hence, one-eighth models could be used, as shown in Fig. 3.. Previous studies from Voth and Packer (2012) and van der Vegte et al. (2010) confirmed the use of hexahedral elements as an appropriate way to describe welded RHS connection behaviour under static loading. Hence brick elements, with three degrees of freedom per node, and reduced integration and hourglass control, were utilized, which are also suitable for nonlinear analysis.

Table 2. FE sensitivity study for specimen X-1.0-21-500O

Element type	No. of elements	No. of nodes	μ	thickness elements	Mesh type	$N_{1,exp.}$ [kN]	$N_{1,}$ [kN]$_{FE}$	$N_{1,exp}$ / $N_{1,FE}$
SOLID185	85 851	100 978	0.1	4	Coarse	1264	1277	0.99
SOLID185	**85 851**	**100 978**	**0.3**	**4**	**Coarse**		**1310**	**0.96**
SOLID185	85 851	100 978	0.5	4	Coarse		1334	0.95
SOLID185	85 851	100 978	0.7	4	Coarse		1349	0.94
SOLID185	31 819	39 960	0.3	3	Coarse		1275	0.99
SOLID185	54 256	66 172	0.3	3	Medium		1274	0.99
SOLID185	104 131	126 360	0.3	3	Fine		1274	0.99
SOLID185	10 509	14 196	0.3	2	Coarse		1217	1.04
SOLID185	169 404	193 181	0.3	5	Coarse		1322	0.96
SOLID186	10509	47 178	0.3	2	Coarse		1328	0.95
SOLID186	41 259	183 281	0.3	3	Coarse		1338	0.95

The influence of the mesh size, the element type (8-noded brick elements called Solid185 vs. 20-noded brick elements called Solid186 in the ANSYS element library), the friction coefficient μ and the number of elements through the thickness were investigated in a sensitivity study using both tests. Table 2 shows the results for test specimen X-1.0-21-500O. As can be seen in Table 2, mesh density had very little influence on the results, so the coarse mesh density was adopted to reduce the number of elements. The three different mesh sizes are further illustrated in Fig. 4.

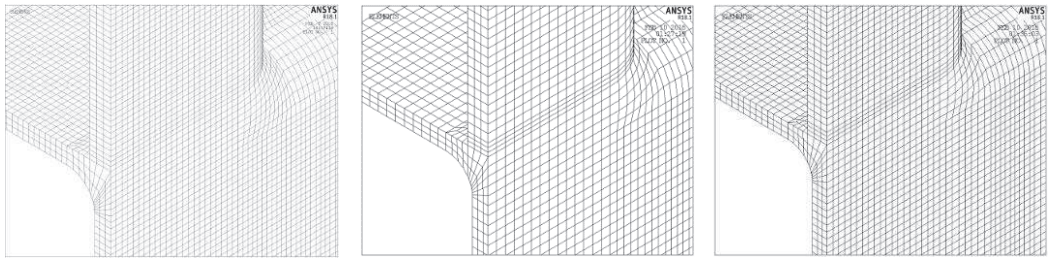

(a) fine mesh (b) coarse mesh (c) medium mesh

Figure 4. FE meshing options examined for RHS-to-RHS connections

A value of 0.3 was taken or the friction coefficient, since this produced the best results compared to the other values for the two experimental tests. Four elements through the thickness using 8-noded elements captured the buckling behaviour of the web well. Using this combination, a comparison of the load-displacement curves between the experiments and the FE model is shown in Fig. 5 and Fig.6. Determination of the connection capacity included consideration of a 3% chord face deformation limit (Lu et al. 1994).

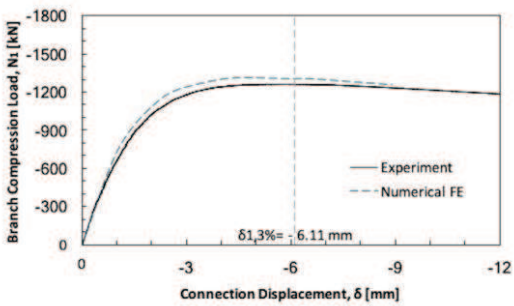

Figure 5. Experimental vs. FE load-displacement curves, X-1.0-21-500O

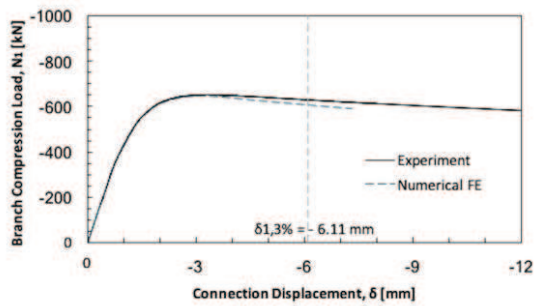

Figure 6. Experimental vs. FE load-displacement curves, X-1.0-32-700O

A parametric study was carried out to produce additional numerical test data and to determine trends/influences of parameters on the connection capacity of full-width welded X-connections. All models used the same material properties, which were extracted from the average tensile coupon tests of the stocky specimen (X-1.0-21-500O). This provided real material behaviour for a cold-formed RHS (Fig. 2). Based on the previously described connection properties, the parametric study included the influences of chord sidewall slenderness (h_0/t_0 from 10 to 50 in steps of 10), chord prestress (n from -0.75, to 0.75 in steps of 0.25), and the branch height-to-chord width ratio (η = 2.0, 1.0, 0.5, 0.25, 0.10). This parameter combination also partially includes the influence of the branch height-to-chord height ratio, h_1/h_0. Two connection arrangements (rectangular and square chords) were created with each having 175 models. The connection ultimate strengths, without chord prestress (n = 0) and normalized by the yield strength $f_{y0}t_0$ $(2h_1 + 10t_0)$, for both arrangements, can be seen in Fig. 7 and Fig.8.

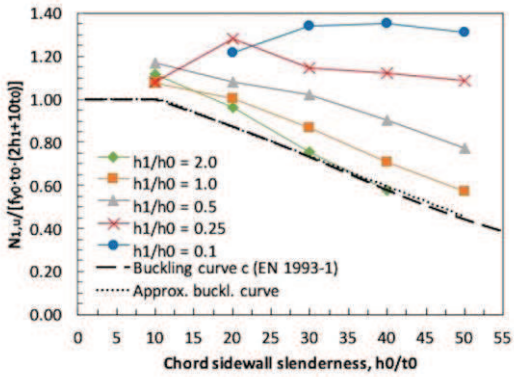

Figure 7. Normalized FE connection strengths, with n = 0, square chord

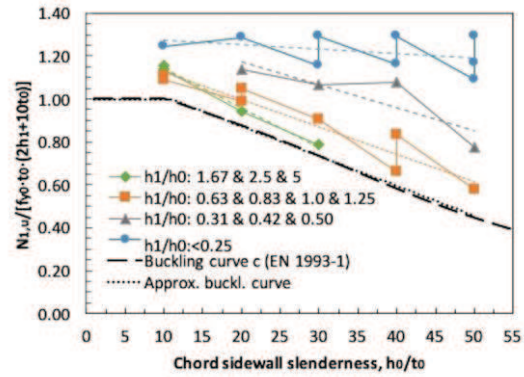

Figure 8. Normalized FE connection strengths, with n = 0, rectangular chord

Both figures clearly show that for a bearing ratio $h_1/h_0 \leq 0.25$ only a negligible reduction of the connection capacity occurs with increasing slenderness of the chord height. The normalization on the vertical axis, as developed by Wardenier (1982), which is based on a load dispersion of 22 °, provides a good description of the bearing behaviour. Further, the buckling behaviour must be described, which occurs for values of h_1/h_0 larger than 0.25. The assumption of the chord web as a pin-ended strut seems to be quite conservative. Since both ends of the chord web are relatively stiff, due to the connecting welds to the branches, fixed-fixed end conditions can be assumed for the equivalent column.

In addition, the effect of tension and compression forces in the chord on the connection capacity was investigated detailed in the parametric study. The connection strength in the presence of a chord preload (compressive and tensile preload), $N_{1,u,preload}$, is plotted normalized by dividing the connection strength with zero preload (n = 0). A comparison to the existing chord stress effect reduction factors, in use by CIDECT DG3 (Q_f) and EN 1993-1-8 (k_n) for these connections, is also shown.

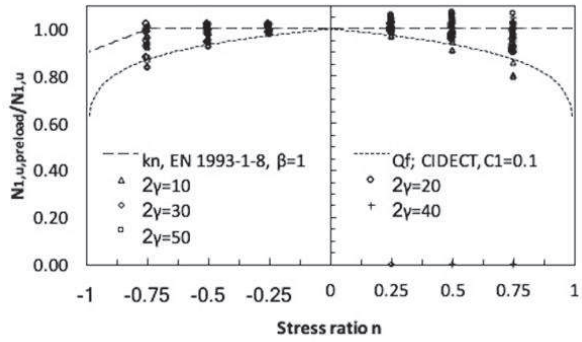

Figure 9. Effect of chord preloading on the strength of full-width RHS-to-RHS X-connections

For stress ratios n between 0 and 1, k_n is generally unconservative whereas Q_f is almost a lower bound. For negative stress ratios, k_n is always unsafe but Q_f describes the influence of compressive preload with a reasonably good function. The need for a new or different Q_f reduction factor is not apparent from the numerical results.

4 Evaluation of Results for Design

The main influence on the connection strength can be assigned to the chord sidewall slenderness ratio (h_0/t_0) and the ratio of bearing length to chord height, ($h_1/\sin\theta_1$)/h_0. Therefore, these parameters must be represented in the design model as well as fixed-fixed end conditions to calculate the buckling reduction factor χ.

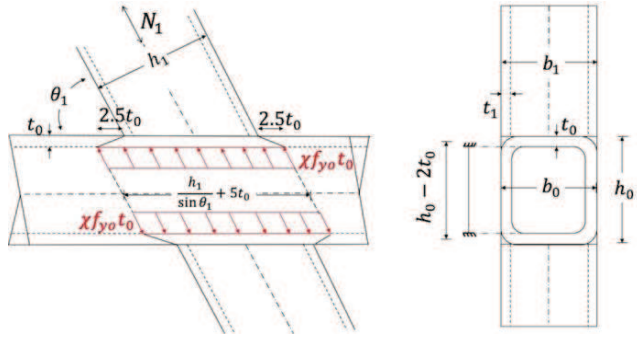

Figure 10. Modified chord wall bearing/buckling model with 1:2.5 load dispersion

The proposed changes of the nominal connection strength are given by:

$$N_1 = 2\chi f_{y0} t_0 \left(\frac{h_1}{sin\theta_1} + 5t_0\right) Q_f \tag{1}$$

where, for $h_1/h_0 \leq 0.25$, $\chi = 1.0$ (yielding) and h_1 is the branch depth. To describe the influence of chord prestress, the factor $Q_f = (1-|n|)^{0.1}$ from the CIDECT Design Guide No. 3 (Packer at al. 2009), is adopted, as this formula has provided a good estimation of the behavior. Assuming fixed-fixed end conditions the non-dimensional slenderness is given by Eq. 2 to determine the buckling factor χ.

$$\lambda = 0.5 \cdot 3.46 \left(\frac{h_0}{t_0} - 2\right) \sqrt{\frac{1}{\sin\theta}} \tag{2}$$

As an alternative, the buckling factor χ can also be approximated with a straight line (Eq. (3)) and generally expressed so that different steel strengths can also be used. However, this is only possible for fixed-fixed end conditions, since otherwise the buckling curve plotted over h_0/t_0 is not nearly straight.

$$\chi = 1.15 - 0.013 \frac{h_0}{t_0} \sqrt{\frac{1}{sin\theta_1}} \sqrt{\frac{f_y}{350}} \leq 1 \tag{3}$$

As a general expression for different yield strength, the term thus can be modified by the term $(f_y/350)^{0.5}$, to generalize the equation. The square roots are taken of both the strength term (fy/350), dependent on the yield strength, and the non-dimensional slenderness term ($1/\sin\theta_1$). Davies et al. (1982) and Packer (1984) found out that the additional term $(1/\sin\theta_1)^{0.5}$ acknowledges increased slenderness for $\theta_1 < 90°$, with the web then considered as an equivalent slanted steel plate. Thus, the term $(1/\sin\theta_1)^{0.5}$ is added to accommodate for the higher slenderness for $\theta_1 < 90°$. An evaluation is performed of the proposed design method, represented by Eq. (1), against both numerical and experimental results. Ultimate strengths r_t and r_e are used in the correlation, where r_t represents the connection theoretical capacity according to the design model, and r_e represents the experimental (as well as the numerical) connection test capacity. Figs. 11 and 12 show the correlation between actual r_e (numerical or experimental tests results) and predicted (theoretical) connection strengths r_t. For the

evaluation of the experimental studies, the "standard procedure" of EN 1990 (DIN, 2010) is applied for experiment-based measurement, in which experimentally determined connection capacities are related to theoretically determined models and evaluated statistically. Based on these evaluations, statements regarding the applicability of the existing design equations for connections in an extended parameter range are possible. The variances of the individual base variables are included in the evaluation as well as the conversion to mean values of the yield stress, according to EN 1990 (DIN, 2010). A detailed description can be found in Kuhn (2018) as well as an example to illustrate the procedure. All numerical data with chord sections classified as Class 1 or 2 were included. A good correlation is shown with numerical tests for RHS-to-RHS connections, with a low coefficient of variation (V_δ) of 0.09. In addition, actual-to-predicted mean values b of 1.17 and 1.28 represent a very economical and accurate prediction of the connection capacity.

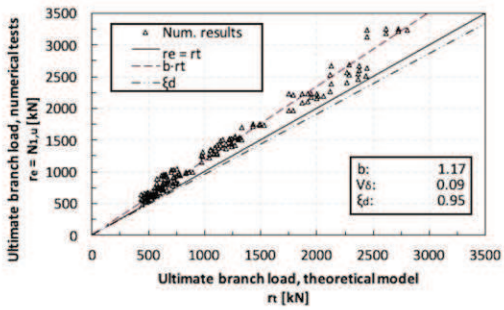

Figure 11. Stat. evaluation of 152 num. test for chord web failure of RHS-to-RHS X-connections

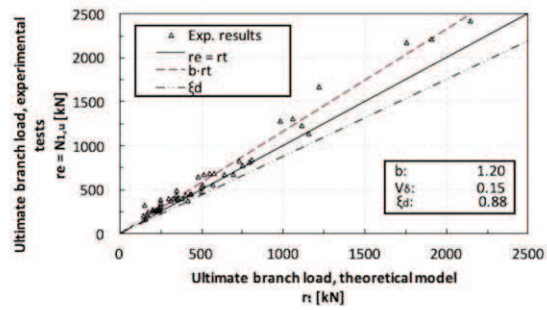

Figure 12. Stat. evaluation of 51 exp. tests for chord web failure of RHS-to-RHS X-connections, for all available tests

5 Conclusion

A large-scale numerical parametric study of full-width ($\beta = 1.0$), welded RHS X-connections was carried out, with the finite element models used being bench-marked against connection tests in the laboratory. The non-linear numerical parametric study included 350 models, covering a wide range of dimensionless geometric variables, and investigated the influence of compressive and tensile preload in the chord on the connection capacity. The reductions of chord preloading (compressive and tensile) were captured very well by the current Q_f formula in CIDECT Design Guide No. 3 (Packer at al. 2009). The connection behaviour of RHS-to-RHS X-connections is strongly dependent on two parameters: the chord sidewall slenderness and the bearing length to chord height ratio, $(h_1/\sin\theta_1)/ h_0$. A critical value $((h_1/\sin\theta_1)/h_0)_{crit} = 0.25$ was found where yielding failure of the chord sidewalls turns into buckling failure, and this has been implemented in the subsequent design recommendation. For fully welded X-connections, and assuming fixed-fixed end conditions, buckling curve c according to EN 1993-1-1 is almost linear when plotted over the practical chord sidewall slenderness range. Therefore, an approximation given by Eq. (3) may be used to determine χ when $(h_1/\sin\theta_1)/h_0 > 0.25$, instead of the λ method. This new design approach for RHS sidewalls under transverse compression outperforms the current CIDECT DG3 model for chord sidewall failure under transverse compression.

Acknowledgments

The Author expresses his gratitude towards his supervisor Professor Jeffrey Packer from the University of Toronto and Prof. K. Tousignant, Dalhousie University for the excellent scientific exchange.

References

AISC. 2016. Specification for structural steel buildings. ANSI/AISC 360-16, American Institute of Steel Construction, Chicago, USA.

CEN. 2005a. Eurocode 3: Design of steel structures – Part 1-8: Design of joints. EN 1993-1-8:2005+AC:2009, European Committee for Standardization, Brussels, Belgium.

Cheng, S., and Becque, J. 2016. A design methodology for side wall failure of RHS truss X-joints accounting for compressive chord pre-load. Engineering Structures, **126**: 689–702.

CSA. 2014. Design of steel structures. CSA S16-14, Canadian Standards Association, Toronto, Canada.

DIN. (2010). Eurocode: Grundlagen der Tragwerksplanung; Deutsche Fassung EN 1990:2002 + A1:2005 + A:2005/AC:2010. Brussels, Belgium: European Committee for Standardization.

Davies, G., and Packer, J.A. 1987. Analysis of web crippling in a rectangular hollow section. Proceedings of the Institution of Civil Engineers, Part 2, **83**: 785–798.

Davies, G., Platt, J.C., and Snell, C. 1982. The buckling of long simply supported rectangular plates under partially distributed skew pinch loads. Report NUCE/ST/10-1982, Department of Civil Engineering, University of Nottingham, Nottingham, U.K.

Fan, Y. 2017. RHS-to-RHS axially loaded X-connections offset towards an open chord end. MASc thesis, University of Toronto, Toronto, Canada.

ISO. 2013. Static design procedure for welded hollow section joints – Recommendations. ISO 14346, International Organization for Standardization, Geneva, Switzerland.

Kuhn, J. 2018. Numerical study of full-width, RHS-to-RHS, X-connections under transverse compression. MASc thesis, Karlsruher Institute of Technology, Germany

Lu, L.H., de Winkel, G.D., Yu, Y., and Wardenier, J. 1994. Deformation limit for the ultimate strength of hollow section joints. *In* Proceedings of the 6th International Symposium on Tubular Structures, Melbourne, Australia, pp. 341–347.

Packer, J. A. 1984. Web crippling of rectangular hollow sections. Journal of Structural Engineering, American Society of Civil Engineers, **110**(10): 2357– 2373.

Packer, J.A. 1987. Review of American RHS web crippling provisions. Journal of Structural Engineering, American Society of Civil Engineers, **113**(12): 2508–2513.

Packer, J. A., Wardenier, J., Zhao, X.-L., van der Vegte, G. J., and Kurobane, Y. 2009. Design guide for rectangular hollow section (RHS) joints under predominantly static loading. CIDECT Design Guide No. 3, 2nd ed. CIDECT, Geneva, Switzerland.

Serrano, M.A., Lopez-Colina, C., Lozano, M., and Iglesias, G. 2017. CUVIPIMECO characterisation of I-beam to RHS-column joints, CIDECT Report 5CE, University of Oviedo, Gijon, Spain.

Swanson Analysis Systems. 2017. ANSYS ver. 18.0. Houston, USA.

van der Vegte, G.J., Wardenier, J., and Puthli, R.S. 2010. FE analysis for welded hollow-section joints and bolted joints. Structures and Buildings, Proceedings of the Institution of Civil Engineers, **163**(6): 427–437.

Voth, A. P., and Packer, J. A. 2012. Numerical study and design of T-type branch plate-to-circular hollow section connections. Engineering Structures, **41**: 477–489.

Wardenier, J. 1982. Hollow section joints. Delft University of Technology, Delft, The Netherlands.

Wardenier, J., Packer, J.A., Zhao, X.-L., and van der Vegte, G.J. 2010. Hollow sections in structural applications, 2nd ed. CIDECT, Geneva, Switzerland.